Topology and Spin Alignment in Organic High-Spin Molecules

Yoshio Teki, Kazunobu Sato, Masayuki Okamoto, Atsuya Yamashita, Yoji Yamaguchi, Takeji Takui, Takamasa Kinoshita, and Koichi Itoh

Department of Chemistry, Faculty of Science, Osaka City University, Sugimoto 3-3-138, Sumiyoshi-ku, Osaka 558, Japan

1. Introduction

Organic high-spin molecules are ideal model compounds for organic magnetic materials such as organic superpara- and ferro-magnets which have recently been attracting increasing interest [1]. The related experimental [2] and theoretical works [3] have been done to serve their molecular design for the last two decades. High-spin polycarbenes as organic high-spin systems, in spite of their highly chemical reactivity, are very important from the view point of organic magnetism as well as of spin ordering/spin control in chemistry from the following reasons. (i) One of the most prominent features of the high-spin polycarbenes is multi-electron open shell systems in the ground or low-lying excited states which arise from degenerate delocalized π orbitals and from σ dangling orbitals localized at divalent carbon atoms, the latter orbitals being nearly degenerate with the highest half-filled π orbitals. (ii) The degeneracy of their π orbitals is governed by a particular connectivity of π electron network, i.e. by the topology of the π electron network.

We have been studying a series of high-spin polycarbenes as well as their π topological isomers [2a,2c,4-19] which are designed by exploiting their π electron networks. We define a π-topological isomer as a molecule which differs from others only in the topology of its π electron network, i.e. in the linking positions of its π bonds. These high-spin carbenes have been successfully detected up to a tridecet polycarbene having twelve parallel spins (S=6) by means of ESR spectroscopy [18].

In this work, we have studied the spin density distributions of high-spin polycarbenes and their topological isomers, biphenyl-n,n'-bis(phenylmethylene) (I: n,n'=3,3'; II: n,n'=3,4') and m- and p-phenylenebis(phenylmethylene), in order to clarify the mechanism of the spin correlation and its role in the intramolecular spin alignment of organic systems.

2. Topological Isomers and Their Spin States

Figure 1 shows the ground states and the low-lying excited states of the high-spin polycarbenes and their topological isomers studied in this work. They were determined from our previous ESR experiments [2a,5,15, 17]. Molecule I has a unique spin alignment in that it has low-lying high-spin states (S=1 and S=2) above the low-spin ground state (S=0) as shown in this figure. In contrast, its topological isomer II has the high-spin ground state. Both molecules have four unpaired electron spins in their nearly degenerate nonbonding π and σ orbitals. On the other hand, molecule III is the first organic high-spin system with the quintet ground state (S=2) [2a], while its topological isomer IV has the low-spin ground state and the low-lying triplet excited state located ca. 200 cm^{-1} above the ground state.

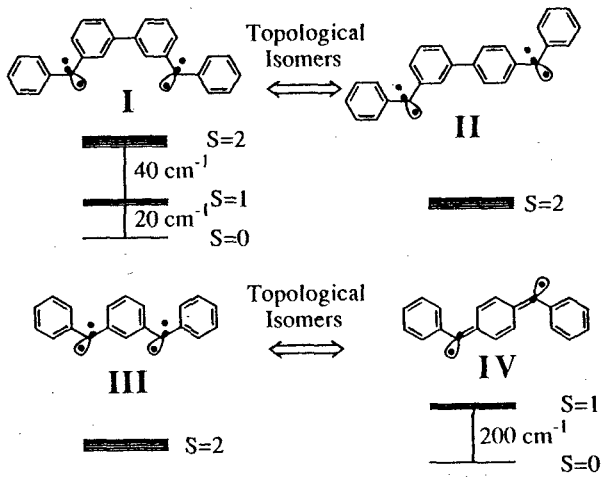

Figure 1. Topological Isomers and their spin states

3. Experimental

The syntheses of the diazo precursors of III and IV were carried out according to the literatures [20,21]. The synthetic work of the carbon 13 labeled compounds of biphenyl-3,3'-bis(phenylmethylene) and other precursors will be published elsewhere. Each diazo precursor was diluted in a host single crystal of benzophenone-d_{10}. Mixed single crystals were grown in the dark by slowly cooling an ethanol or an ether solution containing the diazo precursor. The polycabenes were generated at 2 - 4 K by the photolysis of the corresponding diazo precursors. The photolysis was carried out with an XBO 500W high pressure mercury lamp using a quartz rod which guided the 405 nm light into an X-band TM_{011} ENDOR cavity. All the EPR and ENDOR spectra were recorded with a Bruker ESP 300/350 spectrometer equipped with an Oxford variable temperature controller ESR910. The spectra of the low-lying excited states were observed under the thermal excitation of these levels. Other spectra were measured at ca. 2 - 4 K.

4. Theoretical

In addition to the ENDOR work, we have calculated the spin density distributions of molecules I - VI using two model Hamiltonian approaches. The following unrestricted Hartree-Fock calculation based on a generalized Hubbard model [8] as well as the exact numerical solution of a valence-bond Heisenberg Hamiltonian [9] have provided rather satisfactory and complementary descriptions for spin structures of organic high-spin polycarbenes.

The generalized Hubbard model Hamiltonian is given by [22]

$$\mathcal{H} = -T \sum_{m,m',\sigma} a^{\dagger}_{m',\sigma} a_{m,\sigma} + (U/2) \sum_{m,\sigma} n_{m,-\sigma} n_{m,\sigma} - J \sum_{k,m} [S^z_k S^z_m + (S^+_k S^-_m + S^-_k S^+_m)/2] \quad (1)$$

with $n_{m,\sigma} = a^{\dagger}_{m,\sigma} a_{m,\sigma}$ and $\sigma = \pm 1/2$. The subscripts m and k refer to the pπ and σ sites, respectively. T is the π electron transfer integral between adjacent carbon sites, and U and J are the effective on-site Coulomb repulsion and the exchange integral between the σ and π electrons at the divalent carbon atoms, respectively. In this calculation, these parameters were taken as $U/T = 2.0$ and $J/T = 0.25$, the values of which we have shown to be most appropriate for a series of high-spin polycarbenes such as m-phenylenebis-(phenylmethylene).

As an improved theoretical approach which takes the spin correlation of many open-shell electrons in the polycarbenes into account, we have attempted to obtain an exact numerical solution of the valence-bond Heisenberg Hamiltonian [9,23]:

$$\mathcal{H} = -2 \sum J_{ij}^{eff} \boldsymbol{S}_i \cdot \boldsymbol{S}_j , \quad (2)$$

where J_{ij}^{eff} is the effective exchange integral approximately given by

$$J_{ij}^{eff} = -2|T_{ij}|^2/U_{ii} + J_{ij} . \quad (3)$$

We have estimated $J_{\pi\pi}^{eff} = -1.5$ eV and $J_{\sigma\pi}^{eff}/J_{\pi\pi}^{eff} = -0.2$ [9]. The Heisenberg valence-bond Hamiltonian has exactly been solved by a numerical diagonalization of the matrix derived from the full basis set of the spin system $|S^z_1\ S^z_2\ S^z_3\ \ldots\ S^z_N\rangle$, which the subscript denotes carbon sites.

5. Analysis of ENDOR Spectra

The angular dependence of the ENDOR transitions was measured for the rotation of the magnetic field in the three crystallographic planes, ab, bc, and ca, of benzophenone host single crystals (space group: $P2_12_12_1$, Z=4). From the first-order analysis of the angular dependence, we first obtained the crude hyperfine tensors, and then refined them by comparing the observed ENDOR frequencies with the calculated values obtained by a numerical diagonalization of the matrix of the spin Hamiltonian:

$$\mathcal{H} = \beta_e \boldsymbol{H} \cdot \boldsymbol{g} \cdot \boldsymbol{S} + \boldsymbol{S} \cdot \boldsymbol{D} \cdot \boldsymbol{S} + \sum_i (\boldsymbol{S} \cdot \boldsymbol{A} \cdot \boldsymbol{I}_i - g_N \beta_N \boldsymbol{H} \cdot \boldsymbol{I}_i). \quad (4)$$

All the spin Hamiltonian parameters were determined from this numerical diagonalization of the spin Hamiltonian (4). The π spin density on the carbon site adjacent to the hydrogen atom was obtained from the isotropic term A_F of the hyperfine tensor with the help of McConnell's equation $A_{Fi} = Q\rho_i^{\pi}/2S$, where Q= -66.9 MHz [24] and ρ_i^{π} denotes the π spin density on the i-th carbon site. According to the projection theorem [25], the hyperfine tensor of a state with a total angular momentum S involves the projection factor 1/(2S). We have taken this projection factor into account for the estimation of the π spin densities from McConnell's relation. The spin density is normalized to unity per one unpaired electron. We have also determined the spin densities ρ_j^{π} and ρ_j^{σ} of the π orbital and the σ dangling orbital, respectively, on the j-th divalent carbon atom from the ^{13}C-ENDOR spectra using the equation

$$A_{aniso} = 1/(2S) \left[\begin{pmatrix} -B & & \\ & -B & \\ & & 2B \end{pmatrix} \rho_j^{\sigma} + \begin{pmatrix} -B & & \\ & 2B & \\ & & -B \end{pmatrix} \rho_j^{\pi} \right] \quad (5)$$

where A_{aniso} is the anisotropic term of the ^{13}C hyperfine tensor and B = -89.0 MHz.

6. Results and Discussion

(A) ESR, ENDOR and Spin Density Distribution of Molecule I

The lowest energy levels of biphenyl-3,3'-bis(phenylmethylene) (molecule I) were found to be nearly degenerate singlet, triplet and quintet states in the order of increasing energy, i.e. the singlet ground state [5], as shown in figure 1. The low-lying triplet and quintet spin states locate above the singlet ground state at ca. 20 cm^{-1} and ca. 60 cm^{-1}, respectively. The fine-structure parameters and the g values were determined to be D_T=-0.2958 cm^{-1}, E_T=0.0603 cm^{-1}, and g= 2.004 (isotropic) for the triplet state, and D_Q=0.1035 cm^{-1}, E_Q=-0.0146 cm^{-1}, and g=2.004 (isotropic) for the quintet state, respectively.

No EPR signal of molecule I was observed at 4 K after photolysis. With increasing temperature, the signals due to the triplet state (T_+ and T_-) first appeared at ca. 10 K and then those due to the quintet state (Q_{A+}, Q_{B+}, Q_{B-}, Q_{A-}) appeared at a higher temperature. Figure 2(a) shows a typical EPR spectrum observed at 34 K with the external magnetic field applied parallel to the crystallographic *a* axis of the benzophenone-d_{10} host single crystal. The $T_{\pm}$ lines were assigned to the $\Delta Ms = \pm 1$ allowed transitions of the triplet state and $A_{\pm}$ and $B_{\pm}$ to the allowed transitions corresponding to the $Ms = \pm 2 \leftrightarrow \pm 1$ and $\pm 1 \leftrightarrow 0$ transitions of the quintet state, respectively.

^{1}H- and ^{13}C-ENDOR were measured for the thermally excited triplet state. Figures 2(b) and 2(c) show the typical ^{1}H- and ^{13}C-ENDOR spectra observed at 15 K, respectively, by monitoring the T+ EPR transition in figure 1. We also measured the ^{1}H-ENDOR spectra of the deuterium labeled compound of I in which all the protons in

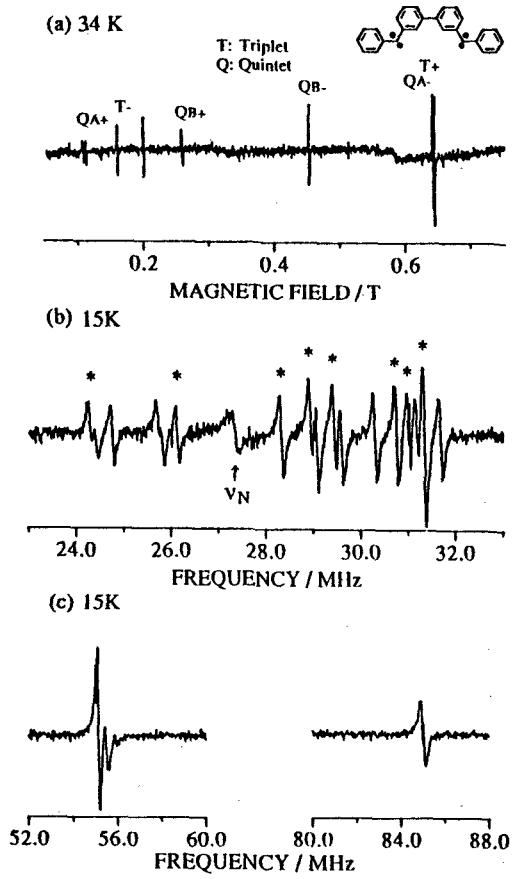

Figure 2. Typical EPR, ^{1}H- and ^{13}C-ENDOR spectra of molecule I. (a) EPR spectrum. (b) ^{1}H-ENDOR spectrum (c) ^{13}C-ENDOR spectrum. The external magnetic field is along the *a* axis. The microwave frequency ν is 9413.0 MHz for the spectra (a) and (b), and 9456.0MHz for the spectrum (c) of the carbon 13 labeled compound, respectively.

the two end phenyl groups were deuterated, in order to facilitate the assignment of ^{1}H-ENDOR transitions by the reduction of the spectral density. By a comparison of the ^{1}H-ENDOR spectra of the deuterium labeled compound with those of the normal compound, the eight transitions labeled by the asterisk in figure 2(b) were assigned to the protons of the central biphenyl group and the remaining unlabeled transitions to those of the end phenyl groups. Thus, we have achieved reliable assignment for all the ^{1}H-ENDOR signals observed.

On the basis of the assignment above, we have determined the π spin densities on the carbon sites adjacent to the hydrogen atoms and the π and σ spin densities on each divalent carbon atom from the analysis of the angular dependence of the ENDOR frequencies as described in section 5. The experimentally obtained spin densities are given in figure 3(a). The spin densities on the six carbon atoms without circles could not be obtained, since they have no adjacent protons.

We have also calculated the spin density distribution theoretically by two model Hamiltonian approaches [8,9,19] as described in section 4. The calculated spin density distribution based on the generalized Hubbard model is shown in figure 3(b). In this calculation, we used the weakly interacting model in which molecule I, biphenyl-3,3'-bis(phenylmethylene), is regarded as composed of two diphenylmethylene moieties, unit A and unit B, weakly interacting with each other. This model has shown to interpret well the observed particular relationship $D_T = -3D_Q$, as described in our previous work [5]. We have applied this model to account for the spin density distribution of molecule I. The spin densities ρ(S,Ms) in molecule I can be derived from $\rho^0(S_A=1,Ms=1)$ of the isolated triplet diphenylmethylene moieties using the equation [15,19]

$$\rho(S=1,Ms=1)_i = (1/2)\rho^0(S_A=1,Ms=1)_i \quad (6)$$

for the triplet state, and

$$\rho(S=2,Ms=2)_i = \rho^0(S_A=1,Ms=1)_i \quad (7)$$

for the quintet state. Similar expressions hold also for unit B since A and B are equivalent. The spin densities of the isolated diphenylmethylene moieties were obtained from the UHF calculation based on the generalized Hubbard model.

This calculation well interprets the ENDOR results as shown in figure 3. The observed and calculated spin density distributions show that the sign of the π spin density is alternatively distributed on the carbon sites within the diphenylmethylene moiety, thus forming the up-and-down

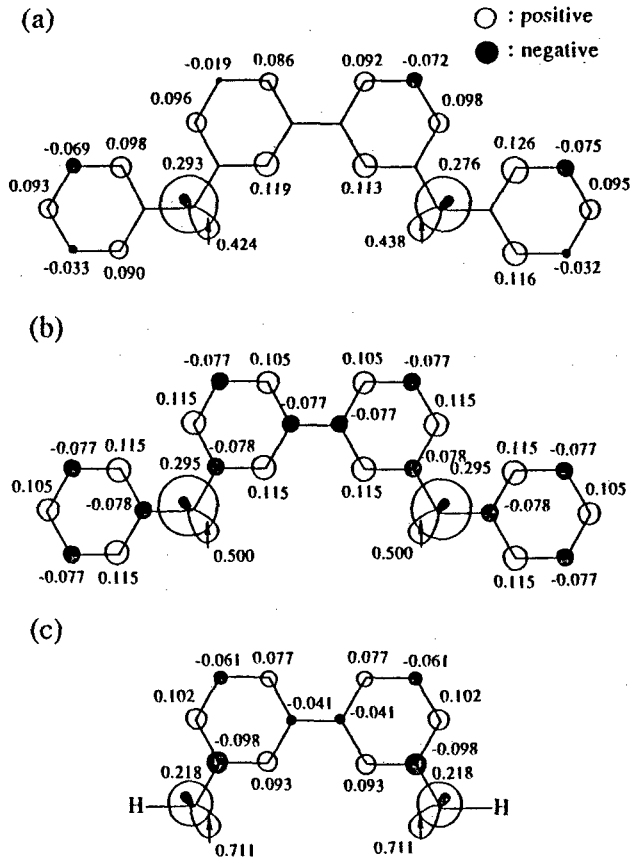

Figure 3 Spin density distribution of the thermally excited triplet state of molecule I. (a) Experimental values, (b) Theoretical values obtained from the UHF generalized Hubbard calculation based on the weakly interacting model. (c) Theoretical values obtained by the valence-bond Heisenberg Hamiltonian approach.

network of the π spin. We define the up-and-down network of the π spin as the pseudo spin density wave (pseudo-SDW), since in infinite systems the up-and-down spin network forms a spin density wave. This network resulting from spin correlation is most favorable in view of the total spin energy (the sum of the spin exchange-correlation energy). The observed spin density distribution is, in principle, symmetrical with respect to the center of the molecule as predicted by the weakly interacting model above. Thus, the pseudo π-SDW is formed within each diphenylmethylene moiety. As a result of these, the central two carbon sites of the biphenyl group (the bridged carbons) should have the same (negative) sign. This violates the up-and-down pseudo π-SDW in the whole molecule, resulting in a node of spin density distribution at the central bridged carbons. The existence of this node, which unstabilizes the spin-correlation energy, makes the observed triplet state to be an excited state above the spin-less ground state. A similar spin distribution is also expected for the quintet state from the comparison of eqs. (6) and (7).

Figure 3(c) shows the spin density distribution calculated by the Heisenberg model Hamiltonian approach where we replaced the end phenyl groups of molecule I with the hydrogen atoms to reduce the dimensionality of the Hamiltonian matrix. In this calculation, we have obtained the results similar to figure 3(b) without using the weakly interacting model. In this approach, the spin correlation is exactly taken into account within the Heisenberg model, leading to the correct ordering of the ground state and the low-lying excited states [9,11].

(B) ESR, ENDOR and Spin Density Distribution of Molecule II]

As mentioned above, the lowest spin ground state, i.e. the singlet ground state, is realized in molecule I, since the high-spin states are unstabilized because of the existence of the node at the central bridged carbons of the biphenyl group. However, if the position of the bridge is shifted by one carbon site as shown in figure 5, it is expected that the nodeless pseudo π-SDW is formed in the whole molecule, leading to the high-spin ground state as a result of the stabilization of spin correlation energy. In order to confirm this, we have observed the ^{1}H-ENDOR spectra of biphenyl-3,4'-bis(phenylmethylene) (molecule II). It was shown by our previous ESR experiments that the ground state of molecule II was a high-spin (S=2) state without low-lying excited states [17]. The fine structure parameters and the g value of the quintet ground state were determined as D=+0.1250 cm^{-1}, E=-0.0065 cm^{-1}, and g=2.003 (isotropic). Figures 4(a) and (b) show a typical ESR and ^{1}H-ENDOR spectra of the quintet ground state of molecule II observed at 2.7 K. The ENDOR spectrum was obtained by monitoring the B_+ ESR transition (Ms=0↔+1). Three transitions by o in figure 4(b) correspond to the ^{1}H-ENDOR signals arising from the Ms = 0 spin sublevel and the remaining unlabeled signals to those from the Ms=+1 sublevel. The eight transitions labeled by the asterisk are due to the protons of the central biphenyl group.

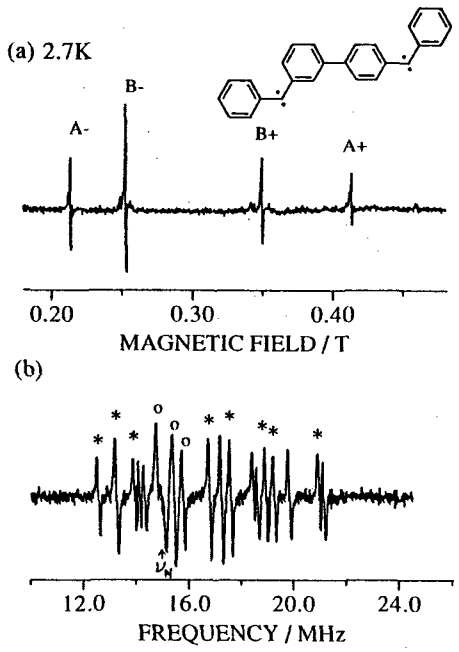

Figure 4. Typical ESR and ^{1}H-ENDOR spectra of molecule II. (a) ESR spectrum. (b) ^{1}H-ENDOR spectrum. The external magnetic field is along the *b* axis. The microwave frequency ν is 9378.7 MHz.

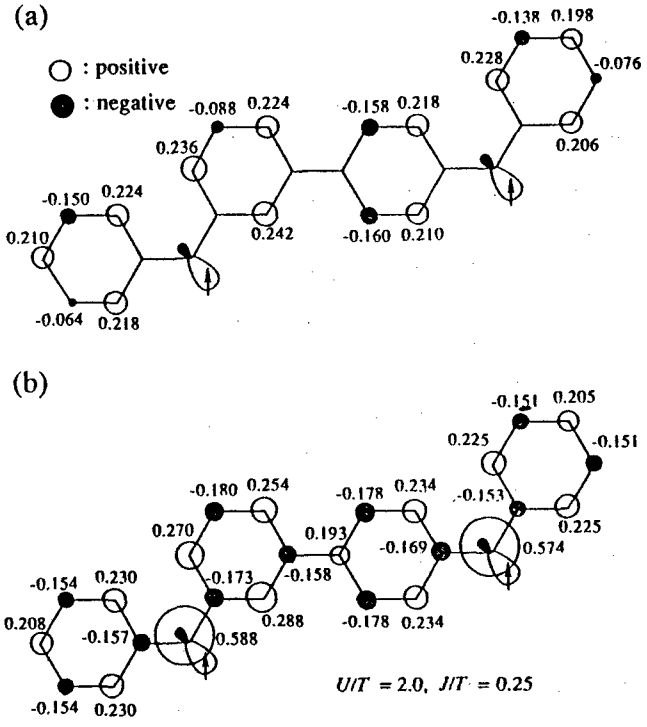

Figure 5 Spin density distribution of the quintet ground state of molecule II. (a) Experimental values. (b) Theoretical values obtained from the UHF generalized Hubbard calculation.

The spin densities obtained from McConnell's equation $A_{Fi} = Q\rho_i^{\pi}/2S$ and the theoretical values calculated on the basis of the Hubbard model are given in figures 5(a) and 5(b), respectively. The observed and calculated spin density

distributions indicate that the nodeless pseudo π-SDW is formed in the whole molecule as expected from the topology of the π electron network of molecule II.

These findings give the following physical picture for the intramolecular spin alignment of molecule II : The unpaired π electrons are distributed over the carbon skeleton with alternating the sign of the spin density from carbon to carbon, thus forming the pseudo SDW in the π electron network. On the other hand, the two unpaired σ spins in the localized σ dangling orbitals become parallel to each other as a results of the ferromagnetic coupling to the unpaired π spins at each divalent carbon site, since the one-center exchange integral J in eq. (3) between the nearly degenerate σ and π orbitals on the same carbene site is usually ferromagnetic. Thus, this picture shows that the spin alignment in molecule II is predominantly determined by the formation of the pseudo π-SDW.

(C) ESR, ENDOR and Spin Density Distribution of Molecule III and IV

To demonstrate the role of spin correlation as determined by the topology of π electron networks, we have also investigated the spin density distribution in the quintet ground state (S=2) of the first organic high-spin molecule, m-phenylenebis(phenylmethylene) III, and that in the low-lying excited triplet state (S=1) of its topological isomer, p-phenylenebis(phenylmethylene) (molecule IV). In the previous work, we reported ESR studies for III and IV [2a,5] and ^{1}H-ENDOR experiments for III [2c]. Figures 6(a) and 6(b) show typical ESR and ^{1}H-ENDOR spectra of III observed at 2 K. The signals labeled by the circle (o) in the ESR spectrum are those due to a minor byproducts. The primed pairs A'± and B'±, and the unprimed pairs A± and B± arise from the two magnetically nonequivalent sites occupied by the guest molecule III in the host single crystal.

A typical ^{13}C-ENDOR spectrum is shown in figure 6(c). We have roughly estimated the π and σ spin densities at each divalent carbon atom from the angular dependence of the ^{13}C-ENDOR frequencies in figure 6(c); the complete analysis by the numerical diagonalization of the spin Hamiltonian (4) is in progress. The anisotropy of the ^{13}C hyperfine tensor is about one half of that of diphenylmethylene reported by Hutchison et al. [26]. This is due to the projection factor 1/(2S) in eq. (5). Our preliminary results indicate that the spin densities on both divalent carbons have values similar to those of diphenylmethylene. Thus, the sign of the spin densities on each divalent carbon site is determined to be positive as expected from the topology of the π electron network of III, and their π spin densities were estimated to be similar in magnitude. The π spin densities on the other carbon sites having adjacent protons were also determined from the isotropic term of each proton hyperfine tensor using McConnell's relation. The spin-density distribution experimentally determined showed that the pseudo π-SDW is formed in the π electron network in a manner similar to the ground state of II.

A question arises as for the low-lying triplet excited state of IV whether there exists a node in the π spin distribution, since II and IV have similar spin structures, i.e. low-lying high-spin excited states above the low-spin (singlet) ground state (figure 1). To answer this question, we measured the ^{1}H-ENDOR spectra of the low-lying triplet excited state of p-phenylenebis(phenylmethylene) (molecule IV). Its typical ESR and ^{1}H-ENDOR spectra are shown in figures 7(a) and 7(b), respectively. The spin density distribution obtained from the analysis of the angular dependence of the ENDOR signals is given in figure 7(c). This shows that the four carbon sites in the central phenyl ring have the same negative sign in the π spin density, leading to a node in the π spin density distribution in the central ring. This finding confirms the physical picture for the formation of low-lying high-spin states above a low-spin/spin-less ground state in topological isomers of high-spin polycarbebes, as described in section 6(A): The node of the spin distribution violates the formation of the pseudo π-SDW in the whole molecule. This unstabilizes the spin correlation energy, leading to the observed triplet state above the singlet ground state.

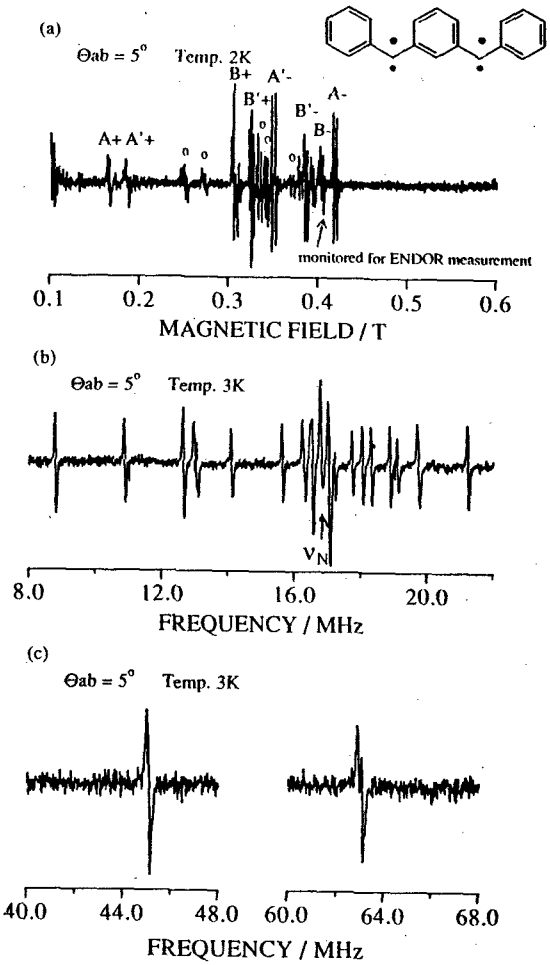

Figure 6. Typical ESR, ^{1}H- and ^{13}C-ENDOR spectra of molecule III. (a) ESR spectrum. (b) ^{1}H-ENDOR spectrum. (c) ^{13}C-ENDOR spectrum. The external magnetic field is along Θ_{ab}= 5° from the *a* axis. The microwave frequency ν is 9430.4 MHz.

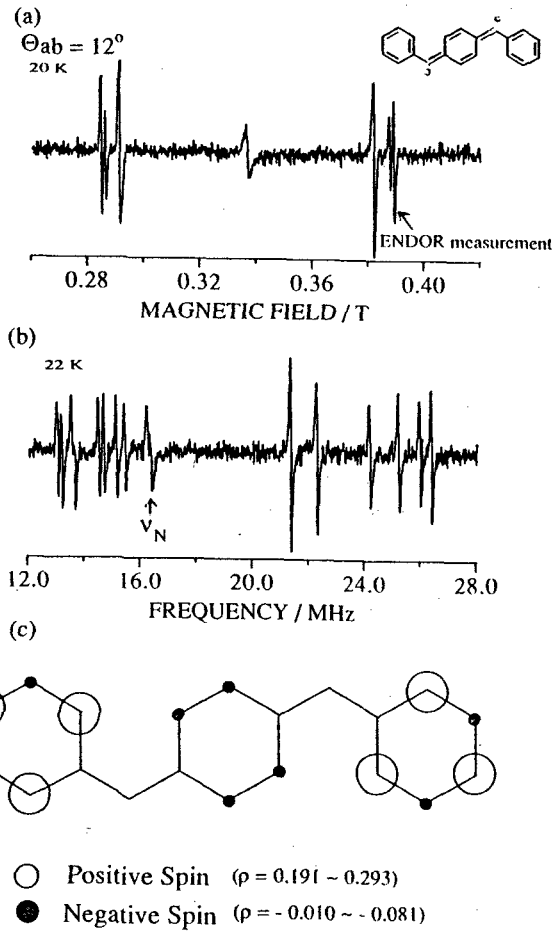

Figure 7. Typical ESR and ^{1}H- ENDOR spectra and spin density distribution of the low-lying triplet excited state of molecule IV. (a) ESR spectrum. (b) ^{1}H-ENDOR spectrum. The external magnetic field is along Θ_{ab}= 12° from the *a* axis. The microwave frequency ν is 9457.0 MHz. (c) Experimentally determined spin densities.

7. Conclusions

We have investigated the spin alignment in the ground states and the low-lying excited states of the high-spin polycarbenes and their topological isomers shown in figure 1. Their spin density distributions were determined by single-crystal ^{1}H- and ^{13}C-ENDOR as well as by the theoretical calculations using the two model Hamiltonians (the generalized Hubbard model and the valence-bond Heisenberg model). The results obtained in this work can be summarized as follows: (1) It is shown that the spin alignment is highly dependent on the topological nature in the π electron network. (2) The pseudo π-SDW governed by the topological nature plays an important role in the stabilization of the high-spin ground state. (3) The spin correlation also plays essential part for the formation of the low-lying spin states of molecule I and IV, as well as of the high-spin ground states of molecule II and III. (4) The physical picture of the intramolecular spin alignment in polycarbenes has been clarified in view of spin correlation.

8. References

1. J.S. Miller and D.A. Dougherty, eds., Proceedings of the symposium on Ferromagnetic and High-Spin Molecular Based Materials, 197th ACS Meeting, Dallas, USA (April 9-12, 1989); Mol. Cryst. Liquid Cryst. **176**, 1-562 (1989).
2. (a) K. Itoh, Chem. Phys. Lett., **1**, 235 (1967). (b) E. Wasserman et al., J. Am. Chem. Soc., **89**, 5076 (1967). (c) T. Takui, S. Kita, S. Ichikawa, Y. Teki, T. Kinoshita, and K. Itoh, Mol. Cryst. Liquid Cryst., **176**, 67 (1989), and references cited therein.
3. (a) K. Itoh, Bussei, 12, 635 (1971). (b) N. Mataga, Theoret. Chim. Acta (Berl.), **10**, 372 (1968). (c) N. Tyutyulkov, G. Olbvich, H. Brenzen, O. Polansky, Theoret. Chim. Acta, **73**, 27 (1988), and references cited therein.
4. T.Takui and K. Itoh, Chem. Phys. Lett.,**19**, 120 (1973).
5. K. Itoh, Pure & Appl. Chem., **50**, 1251 (1978).
6. Y. Teki, T. Takui, K. Itoh, and H. Iwamura, J. Chem. Phys., **83**, 539 (1985).
7. Y. Teki, T. Takui, K. Itoh, H. Iwamura, and K. Kobayashi, J. Am. Chem. Soc., **108**, 2147 (1986).
8. Y. Teki, T. Takui, T. Kinoshita, S. Ichikawa, H. Yagi, and K. Itoh, Chem. Phys. Lett., **141**, 201 (1987).
9. Y. Teki, T. Takui, M. Kitano, and K. Itoh, Chem. Phys. Lett., **142**, 181 (1987).
10. Y. Teki, T. Takui, and K. Itoh, J. Chem. Phys., **88**, 6134 (1988).
11. K. Itoh, T. Takui, Y. Teki, and T. Kinoshita, J. Mol. Electronics, **4**, 181 (1988).
12. K. Itoh, T. Takui, Y. Teki, and T. Kinoshita, Mol. Cryst. Liquid Cryst., **176**, 49 (1989).
13. I. Fujita, Y. Teki, T. Takui, T. Kinoshita, K. Itoh, F. Miko, Y. Sawaki, H. Iwamura, A. Izuoka, and T. Sugawara, J. Am. Chem. Soc., **112**, 4047 (1990).
14. M. Matsushita, T. Momose, T. Sida, Y. Teki, T. Takui, and K. Itoh, J. Am. Chem. Soc., **112**, 4701 (1990).
15. M. Okamoto, Y. Teki, T. Takui, T. Kinoshita, and K. Itoh, Chem. Phys. Lett., **173**, 265 (1990).
16. M. Matsushita, T. Nakamura, T. Momose, T. Sida, Y. Teki, T. Takui, T. Kinoshita, and K. Itoh, J. Am. Chem. Soc., in press (1992).
17. Y. Teki, I. Fujita, T. Takui, T. Kinoshita, and K. Itoh, J. Am. Chem. Soc., submitted (1992).
18. K. Furukawa, T. Matsumura, Y. Teki, T. Kinoshita, T. Takui, and K. Itoh, J. Am. Chem. Soc., submitted (1992).
19. Y. Teki, M. Okamoto, T. Takui, T. Kinoshita, and K. Itoh, J. Am. Chem. Soc., submitted (1992).
20.R. W. Murray and A. M. Trozzolo, J. Org. Chem., **26**, 3109 (1961).
21. S. I. Murahashi, Y. Yoshimura, Y. Yamamoto, and I. Moritani, Tetrahedron, **28**, 1485 (1972).
22. (a)R. M. White, Quantum Theory of Magnetism; Springer, p.139 (1983). (b) K. Nasu, Phys. Rev., **B33**, 330 (1986).
23. S. A. Alexander and D. J. Klein, J. Am. Chem. Soc., **110**, 3401 (1988).
24. N. Hirota, C. A. Hutchison Jr. and P. Palmer, J. Chem. Phys., **40**, 3717 (1964).
25. M. E. Rose, Elementary Theory of Angular Momentum, John Wiley & Sons: New York (1957).
26. C. A. Hutchison Jr., B. E. Kohler, J. Chem. Phys., **51**, 3327 (1979).